Supplementary Information for

A methyl-TROSY approach for NMR studies of high molecular weight DNA with application to the nucleosome core particle

Gili Abramov[1], Algirdas Velyvis[1,2], Enrico Rennella[1], Leo E. Wong[1] and Lewis E. Kay[1,3,*]

[1]Departments of Molecular Genetics, Biochemistry, and Chemistry, The University of Toronto, Toronto, Ontario, M5S 1A8, Canada

[2]Syngenta, Bioscience Department, Jealott's Hill Research Centre, Bracknell, Berkshire RG42 6EY, UK

[3]Program in Molecular Medicine, Hospital for Sick Children, Toronto, Ontario, M5G 1X8, Canada

*Correspondence to: Lewis E. Kay

Email: kay@pound.med.utoronto.ca

www.pnas.org/cgi/doi/10.1073/pnas.2004317117

Materials and Methods

Production of DNA methyltransferases. Synthetic codon-optimized genes for all MTases were cloned into pET-28a(+)-TEV expression vectors (GenScript), with the exception of Dcm and Dam MTases (see below). 6mA and 5mC MTases were transformed into BL21(DE3) and T7 Express *E. coli* cells (New England Biolabs), respectively. The cells were grown in LB/kanamycin media at 37°C to an OD of 0.6-0.8, induced with 1 mM IPTG, with continued growth overnight at room temperature; for Msp expression, the medium was supplemented with 180 g/L D-sorbitol and 2.5 mM glycine betaine, and the cells were induced at 15°C. All MTases expressed as inclusion bodies to varying degrees. The 2Bst, 2Mnl, 1Mnl, and Msp enzymes were purified from their soluble fractions, while the CpG MTase (M.SssI) was purified from inclusion bodies and subsequently refolded via rapid dilution from 6 M to 0.1 M guanidinium chloride (GdnHCl) in the presence of 0.2 M L-Arginine. For 1Bst, an N-terminal NusA-tag was added to increase solubility. MTases were purified using a HisTrap HP Ni affinity column and further purified using a Superdex 200 10/300 GL size-exclusion column (GE Healthcare) equilibrated in the following buffers: 50 mM NaPi, 150 mM NaCl, 2 mM DTT, pH 7.4 (1Mnl); 50 mM Tris-HCl, 200 mM KCl, 2 mM DTT, 3 mM NaN_3, pH 8 (2Mnl, CpG, 2Bst); 100 mM sodium phosphate, 200 mM KCl, 2 mM DTT, 0.5 M Arginine, 3 mM NaN_3, pH 7.5 (Msp); 30 mM Tris-HCl, 200 mM KCl, 0.2 M Arginine, 2 mM DTT, 3 mM NaN_3, pH 7.5 (NusA-1Bst). It is worth noting that, in general, it is necessary to optimize salt concentrations for each new MTase as we have observed that many of these enzymes have a tendency to aggregate. The protein fractions were pooled, concentrated to up to ~50 μM (NusA-1Bst was concentrated to 66 μM without noticeable aggregation), and stored at -80°C as 20%-glycerol stocks.

The gene for the Dcm MTase was obtained by PCR amplification from DH5α genomic DNA and subsequently inserted into a pET28 expression plasmid using NEBuilder HiFi DNA Assembly Master Mix. The plasmid sequence was verified. The Dcm plasmid so obtained was transformed into BL21(DE3) cells and Dcm MTase expressed in a similar manner as for the MTases described above. The harvested cells were resuspended in 50 mM Tris-HCl, 0.3 M NaCl, 20 mM imidazole, 3 mM NaN_3, pH 8 buffer and lysed by sonication, with lysates cleared by centrifugation. Dcm MTase was purified on a HisTrap HP Ni affinity column (equilibration buffer: 50 mM Tris-HCl, 0.3 M NaCl, 20 mM imidazole, 3 mM NaN_3, pH 8; elution buffer: 0.1 M NaH_2PO_4, 0.3 M Imidazole, 3 mM NaN_3, pH 7.9). Ni-eluted Dcm was dialyzed overnight against 20 mM K_2HPO_4, 1 mM DTT, 1 mM EDTA, 5% vol. glycerol, pH 7, and was further purified by gel filtration with Superdex 200 resin in 100 mM NaH_2PO_4, 200 mM KCl, 1 mM DTT, 3 mM NaN_3, pH 7.6. All Dcm containing fractions were pooled and stored at -80ºC as 20% glycerol stocks.

We have found that while MTases can be stored at -80^{o}C for long periods of time they are not stable at higher temperatures (such as 4^{o}C over time). Moreover, some enzymes have a tendency to aggregate either during purification or upon thawing, and refreezing of unused amounts of enzyme can lead to loss of activity. We recommend, therefore, to avoid re-freezing (-80^{o}C) of MTases after thawing, and instead to store small aliquots to be used immediately in a methylation reaction.

Finally, the Dam MTase is indigenous to BL21 cells and methylation using this enzyme was achieved via *in vivo* expression of the DNA of interest, without overexpression or isolation of pure quantities of the enzyme.

Production of S-adenosylmethionine synthase (SAMS). The expression plasmid for SAMS was constructed by PCR amplification of the metK gene from DH5α genomic DNA with insertion of the gene into a pET28 plasmid vector. The plasmid sequence was verified by sequencing. The SAMS plasmid was transformed into BL21(DE3) cells, and protein expressed and purified on a HisTrap HP Ni affinity column as described for Dcm MTase above. The Ni-eluted enzyme was dialyzed overnight against 50 mM Tris-HCl, 50 mM KCl, 1 mM EDTA, 1 mM DTT, 10% glycerol, pH 8, followed by further purification by gel filtration over Superdex 200 resin in 50 mM Tris-HCl, 50 mM KCl, 3 mM NaN_3, 1 mM DTT, pH 7.9. SAMS-containing fractions were pooled and stored at 4ºC.

Methylation of oligonucleotides by Dcm, Msp, 2Bst, 1Bst, 2Mnl, 1Mnl MTases

All single-stranded oligonucleotides (except 12-mer$_{Dam}$) were synthesized by Eurofins Genomics, and mixed in a 1:1 molar ratio with the appropriate complementary strand (except symmetrical Msp oligonucleotides used for assignment, see Fig. S1B, which are palindromic) to generate the double stranded DNA molecules used in MTase reactions. The following precursors were mixed together and incubated at 37°C overnight: 0.2 mM of each of the complementary strands, 2 mM ATP, 1 mM $^{13}CH_3$-methionine, 1.35 μM SAMS, 2 μM MTase, and 2 mM DTT in a methylation reaction buffer containing 25 mM Tris-HCl, 30 mM KCl, 10 mM $MgCl_2$, 0.3 mM NaN_3, pH 7.8. At the end of the reaction, the oligonucleotide was purified from the mixture via ion-exchange using a Mono Q HR 5/5 column (GE Healthcare) equilibrated in 50 mM Tris-HCl pH 7.5, 100 mM NaCl, 1 mM EDTA, 1.5 mM NaN_3 and eluted with a linear gradient up to 1 M NaCl over 10 column-volumes of equilibration buffer. The purified DNA was subsequently buffer exchanged to 99.9% D_2O containing 20 mM NaPi pD 6, 0.05% NaN_3, 0.1 mM EDTA for NMR measurements. The methylation reaction of Figure 1 was conducted directly in an NMR

tube using D_2O-based solutions of $^{13}CH_3$-methionine, DTT and methylation buffer. All reagents were mixed and transferred directly to the NMR tube, without further purification.

Preparation of methylated ^{2}H- and ^{1}H-601 DNA, and extraction of methylated 12-mer$_{Dam}$

601 DNA growth and purification. A pUC19 plasmid DNA carrying ~30 copies of 153-bp 601 DNA (kindly provided by the Muir Laboratory, Princeton) was transformed into BL21(DE3) *Escherichia coli* cells and grown in LB/ampicillin to an OD of 1 (37°C). Each of the 30 copies was linked by 12-bp sequences, 12-mer$_{Dam}$, SI Appendix, Figure S2A. Cells were subsequently transferred to either a 1 L LB/ampicillin medium (for fully protonated 601 DNA) or 100 mL of D_2O-based minimal media (for deuterated 601 DNA) to generate an initial OD of ~0.1, and grown overnight at 37°C. The 100 mL overnight D_2O culture was transferred to 900 mL of D_2O minimal media, supplemented with 4 g/L [^{2}H,^{12}C]-glucose and 10 mL of Bioexpress Cell Growth Media (U-D, 98%) (Cambridge Isotope Laboratories), and grown overnight at 37°C to saturation. The cells were harvested by centrifugation, followed by plasmid purification using QIAGEN Giga prep columns. Typical yields from 1 L minimal media ranged between 4 - 6 mg of plasmid DNA. To obtain $^{13}CH_3$-12-mer$_{Dam}$ (Fig. 3), the D_2O medium was supplemented with 100 mg/L $^{13}CH_3$-methionine, without using Bioexpress media.

Plasmid DNA was digested overnight at 37°C using the EcoRV restriction enzyme (0.5 units/µg plasmid) in 50 mM Tris-HCl, 10 mM $MgCl_2$, 1 mM DTT, pH 7.9, liberating copies of 153-bp 601 DNA and 12-mer$_{Dam}$. PEG-8000 was added to the resulting solution to reach 10% (from a fresh 30% PEG-8000 stock solution) and the $MgCl_2$ concentration adjusted to 10 mM. The mixture was left at 4°C for 1 hour to precipitate the vector backbone. Following centrifugation at 14,000 rpm (Beckman JA-20 rotor) for 30 minutes at 4°C, the supernatant containing the DNA fragments was applied to a HiTrap DEAE-FF column (GE Healthcare)

equilibrated in 10 mM Tris-HCl, pH 8 and subsequently eluted using a linear gradient in NaCl (up to 1 M) in over 9 column volumes of the equilibration buffer. Fractions containing DNA were pooled, and further purified by size-exclusion chromatography using a Superdex 200 column, on which the 153-bp 601 and 12-mer$_{Dam}$ fragments were well separated. Each step in the DNA purification process was monitored by agarose gel electrophoresis, as shown in SI Appendix, Figure S2B.

Methylation reaction of 601 DNA. Purified 601 DNA was concentrated and mixed in a one-pot methylation reaction with Msp (5mC), 2Bst (6mA), 1Bst (6mA), and 2Mnl (6mA) MTases. The reaction included 1 mg/mL 601 DNA, 2 mM ATP, 1 mM $^{13}CH_3$-methionine, 1.35 µM SAMS, 2 µM of each of the MTases, and 2 mM DTT in a methylation reaction buffer containing 25 mM Tris-HCl, 30 mM KCl, 10 mM $MgCl_2$, 0.3 mM NaN_3, pH 7.8. The mixture was incubated at 37°C overnight and subsequently applied to a Mono Q HR 5/5 column equilibrated with 50 mM Tris-HCl, pH 7.6, 100 mM NaCl, 1 mM EDTA, 1.5 mM NaN_3 buffer and eluted with a linear gradient up to 1 M NaCl over 10 column-volumes of equilibration buffer. The methylated 601 DNA was buffer exchanged to 99.9% D_2O containing 20 mM NaPi pD 6, 0.05% NaN_3, 0.1 mM EDTA for NMR analysis. Methylation of 601 DNA by CpG MTase (M.SssI) was carried out as described above for the other MTases.

601-DNA methylation reaction goes to completion. 601 DNA samples methylated by Dcm, 2Bst, Msp, 2Mnl and CpG MTases, as well as unmethylated 601 DNA ('control'), were treated with the corresponding restriction endonucleases, PspGI, BtsCI, HpaII, MnlI, and HhaI (New England Biolabs), respectively, using a reaction setup in which 20 µg/mL DNA, 1µL enzyme (stocks ranged from 5,000 to 20,000 units/mL), 1x CutSmart Buffer (NEB) were added to a final

reaction volume of 20 µL. The digestion reaction mixtures were incubated at 75°C (PspGI), 50°C (BtsCI) or 37°C (HpaII, Mn1I, HhaI) for ~15 min (60 min for PspGI), followed by dilution to 36 µL solutions containing a DNA loading dye. 9 µL of each digest solution (corresponding to 0.1 µg DNA) was loaded onto a 7% polyacrylamide gel using 1x Tris-Borate EDTA as running buffer (60 min, 200 V, room temperature). The gels were stained with SafeView^{TM} DNA stain for 10-20 min. Methylated 601 DNA was protected against digestion, while unmethylated 601 DNA was digested as shown in Figure 1 and SI Appendix, Figure S2C (reaction with Dcm, 2Bst, Msp, 2Mnl MTases) and SI Appendix, Figure S3 (reaction with CpG MTase). It is worth noting that for most reactions under our concentration conditions (of methionine, ATP and MTase), an incubation period of 1 to 3 hours at 37°C was sufficient for complete methylation. However, some reactions required an incubation overnight (M. SssI); we chose, therefore, to incubate overnight by default.

Preparation of nucleosome core particle samples

Growth and purification of histones. The genes for histones H2A, H2B, H3 and H4 from *D. melanogaster* were cloned into pET21b expression vectors, as previously published (1). The H3C110S mutant of H3 was used in all NCP samples, prepared as described previously (2). For H2B, an N-terminal his-tag was inserted into the H2B gene, followed by a TEV cleavage site, while all other histones were tagless. We have inserted an Ile at position 0 in the H2B gene (*i.e.*, the Ile is not part of the original H2B sequence) to aid in protein overexpression. Histone proteins were transformed individually into BL21(DE3) cells, and grown in 5 mL LB/ampicillin media to an OD_{600} of 1. The cells were pelleted at room temperature and resuspended in 100 mL D_2O-based minimal medium supplemented with 3 g/L of d_7-glucose. The culture was grown overnight at 37°C and subsequently transferred into 900 mL D_2O-minimal media with continued

shaking until an OD_{600} of ~1 was reached. The cells were then induced with 1 mM IPTG and protein expression was allowed to occur for ~18 hours at 37°C for H2A, His-H2B and H3C110S and ~6 hours at 37°C for H4. Cells were subsequently harvested by centrifugation and resuspended in wash buffer (50 mM Tris-HCl pH 7.5, 100 mM NaCl), followed by immediate purification or storage at -80°C. For ILV-methyl labeling of histone H2B (in a highly deuterated background), the D_2O culture was supplemented with 60 mg/L α-ketobutyric acid (I labeling; $^{13}CH_3CD_2COCOOH$) and 80 mg/L α-ketoisovaleric acid (L/V labeling; ($^{13}CH_3CD_3$)CCOCOOH) one hour prior to induction of protein overexpression with the addition of IPTG. All histones were purified from inclusion bodies: H2A, H3C110S and H4 were purified using HiTrap SP XL ion exchange (IEX) columns (GE Healthcare) equilibrated in 7 M urea, 100 mM NaCl, 50 mM NaPi pH 7.5, 1 mM EDTA and eluted using a linear gradient up to 1 M NaCl over 9 column volumes of the equilibration buffer. H2B was purified using a HisTrap HP Ni affinity column equilibrated with 20 mM NaPi pH 7.5, 0.5 M NaCl, 40 mM imidazole, 6 M GdnHCl and eluted with Ni equilibration buffer containing 500 mM imidazole. The his-tagged histone was then diluted into 20 mM NaPi pH 7.5, 0.5 M NaCl, 2 mM DTT and subjected to TEV cleavage (overnight at 4°C). Cleaved H2B was subsequently eluted on a Ni column using equilibration buffer containing 6 M GdnHCl. IEX histone fractions as well as reverse-Ni H2B fractions were dialyzed extensively into water, lyophilized and stored at -80^{o}C until use. Protein purity was evaluated by SDS-PAGE.

Octamer formation and NCP reconstitution. Lyophilized and purified ^{2}H-H2A, ILV-H2B, ^{2}H-H3C110S and ^{2}H-H4 were dissolved in unfolding buffer (20 mM Tris-HCl pH 7.5, 6 M GdnHCl), combined in equimolar ratios and refolded into octamers, via gradient dialysis into refolding buffer (10 mM Tris-HCl pH 7.5, 2 M NaCl, 1 mM EDTA). Reconstituted octamers

were purified by gel-filtration on a S200 GL 10/300 column equilibrated with refolding buffer. Octamer fractions were pooled and subsequently combined at a 1:1 molar ratio with purified methylated 601 DNA at high salt (2 M KCl). Reconstitution of NCPs was carried out at 4^{o}C by gradient dialysis into 10 mM Tris-HCl pH 7.5, 0.25 M KCl, 1 mM EDTA. Following reconstitution, NCPs were gradually dialyzed into 10 mM Tris-HCl pH 7.5, 1 mM EDTA buffer and finally exchanged into NMR buffer (see below). A detailed octamer refolding and NCP reconstitution protocol has been described by Lugar and coworkers (3).

NMR samples

All NMR samples were dissolved in 20 mM NaPi buffer, pD 6, 0.05% NaN_3, 99.9% D_2O, with the exception of 12-mer$_{Dam}$ where the buffer was 25 mM NaPi, 100 mM NaCl, 90%H_2O/10%D_2O, pH 7.4. Methylated ^{2}H and ^{1}H 601-DNA NMR samples were 222 µM and 249 µM in DNA, respectively, while the 12-mer$_{Dam}$ sample was 45 µM in DNA (all concentrations refer to duplex DNA). A second methylated ^{2}H 601-DNA sample, 130 µM, was used to record the spectrum in Figure 4B. NCP sample concentrations were 148 µM (methylated with 2Bst, 1Bst, 2Mnl, Msp MTases) and 120 µM (methylated with CpG MTase, such that all CpG sites are methylated). Concentrations of all samples were based on A_{260} readings that provide a quantitative measure of the amount of DNA.

NMR experiments

All NMR experiments were recorded on an 18.8 T Bruker Avance III HD spectrometer, equipped with an *x*,y,*z* gradient TCI CryoProbe, with the exception of measurements on the 12-mer$_{Dam}$ sample (Fig. 3) that were almost all recorded on a 14.0 T Bruker Avance III HD spectrometer with a similar cyroProbe configuration as on the 18.8 T magnet. ^{13}C-^{1}H HMQC spectra of the

small oligonucleotides (Fig. 2) and ^{2}H 601 DNA (Fig. 4B) were recorded at 25°C, while relaxation measurements of methyl DNA protons and all studies relating to NCPs were performed at 45°C. All NMR data (see below) were processed and analyzed using the NMRPipe software package (4). Assignments of the ILV methyl groups in histone H2B of the NCP were transferred directly from those previously published (1), while the assignments of methyl groups attached to DNA were obtained through comparison with spectra of oligonucleotides as described in the main text and illustrated in SI Appendix, Figure S1.

T_1 relaxation measurements. Methyl ^{1}H T_1 relaxation times were obtained by recording a series of 2D ^{13}C-^{1}H HMQC spectra of methylated ^{1}H- and ^{2}H-601 DNA. Initially, ^{1}H magnetization was dephased via a spin-lock and 90_x-gradient, 90_y-gradient purge elements, eliminating longitudinal magnetization at T=0. A recovery period of duration T followed, after which the magnetization was 'read out' using an HMQC pulse scheme. Ten relaxation time points, extending from 0.5 s – 8 s were recorded and intensities, $I(T)$, were fit to the relation $I(T)=I_o(1-\exp(-T/T_1))$ and plotted as $I(T)/I_o$ in Figure 6. Errors were estimated via a Monte-Carlo approach (5), taking the deviation between the best-fit and experimental points as a measure of the error.

T_2 relaxation measurements. ^{1}H T_2 relaxation times of methylated ^{1}H- and ^{2}H-601 DNA were measured using a pulse scheme described previously (6) that selects for the slowly relaxing component of methyl ^{1}H transverse magnetization. Ten T delays (during which transverse magnetization decays), ranging from 1.55 ms to 24 ms were recorded, and intensities fit to the relation $I(T)=I_o\exp(-T/T_2)$ and plotted as $I(T)/I_o$ in Figure 5. In a similar manner, ^{1}H T_2 relaxation rates of methylated DNA in the context of NCPs were also obtained, in this case from seven T delays extending from 1.55 ms to 15 ms. Errors were estimated as described for the T_1 data.

^{13}C T_1 relaxation measurements. Estimates of τ_e values, quantifying rates of rotation about the methyl symmetry axis, were obtained using a variant of a 2D CEST-based pulse scheme (7) in which the decay of 'pure' ^{13}C longitudinal magnetization is monitored. Six relaxation points (ranging from 0.05 s to 1.2 s) were recorded on the methylated ^{2}H-601 DNA sample and intensities fit to the relation $I(T)=I_o\exp(-T/T_1)$. Extracted T_1 values ($R_1^C = 1/T_1$) were then used to estimate τ_e from Eq. [2] using r_{HC} = 1.117 Å (8) and S^2_{axis} = 1.

Measuring rapid pico- to nano-second timescale methyl dynamics. $S^2_{axis}\tau_{c,eff}$ values were measured and analyzed for DNA- and H2B-based methyl groups as described previously (9, 10) using an approach in which the sums (I_{SQ}) and differences (I_{3Q}) of single quantum methyl ^{1}H magnetization components are quantified,

$$\left|\frac{I_{3Q}}{I_{SQ}}\right| = 0.75\frac{\eta\tanh(\sqrt{\eta^2+\delta^2}T)}{\sqrt{\eta^2+\delta^2}-\delta\tanh(\sqrt{\eta^2+\delta^2}T)} \qquad [S1]$$

In Eq. [S1] δ measures the ^{1}H spin-density in the vicinity of the methyl group of interest and

$$\eta \approx \frac{9}{10}[P_2(\cos\theta_{axis,HH})]^2\frac{S^2_{axis}\gamma^4_H h^2\tau_{c,eff}}{4\pi^2 r^6_{HH}} \qquad [S2]$$

where γ_H is the gyromagnetic ratio of a ^{1}H spin, r_{HH} is the distance between methyl protons (1.813Å), $P_2(x)=\frac{1}{2}(3\cos^2 x-1)$, h is Planck's constant, and $\theta_{axis,HH}$ (90^o) is the angle between a vector connecting pairs of methyl protons and the methyl 3-fold symmetry axis. Values of I_{SQ} and I_{3Q} were measured for time points of 0.3, 0.7, 1, 1.5, 2, 3,…, 10 ms (13 time points) with 24 and 72 scans for measurements of I_{SQ} and I_{3Q}, respectively, that were recorded in an interleaved manner, resulting in a net acquisition time of approximately 66 h for the pseudo-4D data set.

Methyl-TROSY based CPMG measurements of 12-mer$_{Dam}$. Experiments were recorded with a pulse scheme described previously (11) at static magnetic field strengths of 14.0 T and 18.8 T. A temperature of 48.5^{o}C was chosen so that methyl correlations derived from both single-stranded and double-stranded DNA could be analyzed simultaneously. Although partially resolved peaks were observed for the pair of 6mA methyl groups for the double stranded conformation (Fig. 3A), these were analyzed together (*i.e.*, the intensities of both peaks were summed). A set of 11 ν_{CPMG} values {0.2, 0.3, 0.5, 0.7, 0.8, 1.0 (x2), 1.2, 1.4, 1.7, 2.0} kHz were obtained (1 duplicate for error analysis), in addition to an experiment with the constant-time relaxation element (set to 10 ms) removed. The size of the dispersion profile from the single-stranded DNA increases very significantly from 14.0 T to 18.8 T; only ν_{CPMG} values of {0.8, 1.0 (x2), 1.2, 1.4, 1.7, 2.0} kHz could be included in the analysis of the 18.8 T data, as the intensities of the correlations from the smaller CPMG frequencies were too weak to quantify. Measurement times were ~65 h/pseudo 3D data set. Data were analyzed using the software package *ChemEx* (https://github.com/gbouvignies/ChemEx). In principle multiple-quantum dispersion profiles are sensitive to both $|\Delta\varpi_C|$ and $|\Delta\varpi_H|$ where $\Delta\varpi_j$ is the j chemical shift difference (ppm) between an exchanging spin in ground and excited states. In practice, however, it can be difficult to extract accurate measures for $|\Delta\varpi_C|$ and $|\Delta\varpi_H|$ from fits of only multiple-quantum dispersions without including additional data. We have, therefore, fit our profiles assuming either $\Delta\varpi_H = 0$ ppm or allowing $\Delta\varpi_H$ to float. If the population of the excited state, p_E, is set to 0.10 in the fits, as suggested by previous work (12), we obtain $\Delta\varpi_C \sim 3.5$ ppm, and for the case where $\Delta\varpi_H$ is allowed to float, the best-fit of the data is obtained when $\Delta\varpi_H \sim 0.15$ ppm. As described in the main text, the large dispersion for the methyl groups attached to single-stranded DNA most likely arises from rotation about the C6-N6 bond, as depicted in Figure 3E, which interconverts

the methyl group between *cis* and *trans* conformations. Noting that methyl groups of single-stranded DNA are predominantly in the *cis* conformation (12), while those of duplex DNA are completely *trans* it follows that an estimate for $|\Delta\varpi_C|$ (~ 3 ppm) and $|\Delta\varpi_H|$ (~ 0.2 ppm) can be obtained from the diagonal peak positions in Figure 3C that derive from duplex (blue) or single-stranded (orange) DNA. The fitted values of chemical shift differences (for p_E = 0.1) are thus consistent with expectations based on the exchange model presented.

Magnetization exchange monitoring the kinetics of annealing of 12-mer$_{Dam}$. Magnetization exchange experiments, similar to those described previously (11), were recorded to quantify the rate of duplex$\leftrightarrow$single-strand DNA interconversion. The pulse scheme records ^{13}C chemical shift, followed by a mixing delay during which longitudinal order, I_zC_z, exchanges (where A_z is Z-magnetization from nucleus A), and subsequently ^{1}H chemical shift is recorded during direct detection. A pseudo-3D data set was obtained with 6 mixing times {50, 100, 200, 300, 400, 500}ms (~ 26 h) and analyzed as described below and in Farrow *et al*. (11).

Using molecular dynamics simulations for isolating S^2_{axis} values from $S^2_{axis}\tau_{c,eff}$

An average rotational diffusion tensor of the NCP from Xenopus laevis (PDB 3LZ0, (13)) based on a series of snap-shots of a molecular dynamics trajectory was kindly provided to us by Professor Nikolai Skrynnikov (Purdue University) and Dr. Sevastyan Rabdano (Laboratory of Biomolecular NMR, St. Petersburg State University). The matrix so obtained (in units of s^{-1}) is

$$\boldsymbol{D} = \begin{bmatrix} 1638125.4 & 52705.5 & -10136.3 \\ 52707.6 & 1277843.0 & -18375.9 \\ -10138.0 & -18375.2 & 1477407.8 \end{bmatrix} \quad [S3]$$

in the 3LZ0 pdb coordinate frame. The NCP was rotated into the principle axis system of $\boldsymbol{D}$ and the pdb of the NCP used in the relaxation measurements (6ESF, (14)) superimposed on the

rotated structure. The direction cosines of each DNA methyl 3-fold symmetry axis (methyl groups were added to the 6ESF structure) with respect to the principle axis system of ***D*** were calculated from which $\boldsymbol{\tau}_{c,eff}$ was evaluated as $\boldsymbol{\tau}_{c,eff} = \frac{1}{2}\sum_{k=1-5} A_k \boldsymbol{\tau}_k$, with the values of A_k and τ_k given in Eq. [3] of Tjandra *et. al.* (15). Note the factor of 1/2 in the sum accounts for a missing factor of 2 in Eq. [3] of that reference. The values of $\boldsymbol{\tau}_{c,eff}$ so obtained are {117.1,118.5,112.1,108.3,119.3}ns for Msp-Top, Msp-Bott, 2Mnl, 2Bst and 1Bst methyl labels, respectively, with $\boldsymbol{\tau}_{c,isotropic}$ = 113.8 ns.

Analysis of the 12-mer$_{Dam}$ magnetization exchange experiment

Consider the following binding reaction,

$$A + B \underset{k_{-1}}{\overset{k_1}{\rightleftarrows}} CD \qquad \text{[S4]}$$

where *A* and *B* are single strands of complementary DNA molecules and *CD* is the double stranded complex. In Eq. [S4], *C* and *D* in complex *CD* denote strands *A* and *B*, respectively. We choose to distinguish between *A* and *C*, as well as between *B* and *D*, because although strands *A* and *C* (or *B* and *D*) are chemically equivalent they are magnetically distinct, in the sense that separate resonances are observed for methyl probes in *A*/*C* and in *B*/*D*. It is straightforward to write a set of kinetic equations for the reaction of Eq. [S4] as

$$\begin{aligned}
\frac{d[A]}{dt} &= -k_1[A][B] + k_{-1}[CD] \\
\frac{d[B]}{dt} &= -k_1[A][B] + k_{-1}[CD] \qquad \text{[S5]} \\
\frac{d[CD]}{dt} &= k_1[A][B] - k_{-1}[CD]
\end{aligned}$$

Following a procedure described previously (16) we can write the reaction of Eq. [S4] in terms of the spin states {α,β} of the 'spy' spin that 'reports' on the exchange process,

$$\begin{aligned} A_\alpha + B_\alpha &\underset{k_{-1}}{\overset{k_1}{\rightleftharpoons}} C_\alpha D_\alpha \\ A_\alpha + B_\beta &\underset{k_{-1}}{\overset{k_1}{\rightleftharpoons}} C_\alpha D_\beta \\ A_\beta + B_\alpha &\underset{k_{-1}}{\overset{k_1}{\rightleftharpoons}} C_\beta D_\alpha \\ A_\beta + B_\beta &\underset{k_{-1}}{\overset{k_1}{\rightleftharpoons}} C_\beta D_\beta \end{aligned} \qquad [S6]$$

from which Eq. [S7] follows

$$\begin{aligned} \frac{d[A_\alpha]}{dt} &= -k_1[A_\alpha][B_\alpha] + k_{-1}[C_\alpha D_\alpha] - k_1[A_\alpha][B_\beta] + k_{-1}[C_\alpha D_\beta] \\ \frac{d[A_\beta]}{dt} &= -k_1[A_\beta][B_\alpha] + k_{-1}[C_\beta D_\alpha] - k_1[A_\beta][B_\beta] + k_{-1}[C_\beta D_\beta] \end{aligned} . \qquad [S7]$$

Combining the two expressions in Eq. [S7] gives

$$\frac{d([A_\alpha]-[A_\beta])}{dt} = -k_1([A_\alpha]-[A_\beta])([B_\alpha]+[B_\beta]) + k_{-1}([C_\alpha D_\alpha]+[C_\alpha D_\beta]-[C_\beta D_\alpha]-[C_\beta D_\beta]). \qquad [S8]$$

Noting that the Z-magnetization from the probe in strand A, M_Z^A, is given by

$$M_Z^A = \frac{\gamma\hbar}{2}([A_\alpha]-[A_\beta]), \qquad [S9.1]$$

while the corresponding Z-magnetization from the probe in strand C of the complex, M_Z^C, is

$$M_Z^C = \frac{\gamma\hbar}{2}([C_\alpha D_\alpha]+[C_\alpha D_\beta]-[C_\beta D_\alpha]-[C_\beta D_\beta]) \qquad [S9.2]$$

it follows that

$$\frac{dM_Z^A}{dt} = -k_1[B]M_Z^A + k_{-1}M_Z^C \qquad [S10]$$

where $[B]=[B_\alpha]+[B_\beta]$.

The time evolution of M_Z^B can be obtained directly from Eq. [S10] by interchanging *A* and *B*, and *C* and *D*. The time evolution of $[C_iD_j]$, $i,j \in \{\alpha,\beta\}$, in turn, is given by

$$\frac{d[C_iD_j]}{dt} = k_1[A_i][B_j] - k_{-1}[C_iD_j] \qquad \text{[S11]}$$

and following a similar process to that above it can be shown that

$$\begin{aligned} \frac{dM_Z^C}{dt} &= k_1[B]M_Z^A - k_{-1}M_Z^C \\ \frac{dM_Z^D}{dt} &= k_1[A]M_Z^B - k_{-1}M_Z^D \end{aligned} \qquad \text{[S12]}$$

so that the coupled set of equations that describe the time evolution of Z-magnetization for the exchanging system under consideration are

$$\begin{aligned} \frac{dM_Z^A}{dt} &= -k_1[B]M_Z^A + k_{-1}M_Z^C \\ \frac{dM_Z^B}{dt} &= -k_1[A]M_Z^B + k_{-1}M_Z^D \\ \frac{dM_Z^C}{dt} &= k_1[B]M_Z^A - k_{-1}M_Z^C \\ \frac{dM_Z^D}{dt} &= k_1[A]M_Z^B - k_{-1}M_Z^D \end{aligned} \qquad \text{[S13]}$$

where we have not included spin relaxation terms that can be added phenomenologically and the terms for equilibrium magnetization have been neglected. As the chemical shifts of the methyl probes in *A* and *B* are degenerate, and methyl probes in *C* and *D* are highly overlapped, we prefer to consider the total magnetization from the single and double stranded DNA, M_Z^{A+B} and M_Z^{C+D}, respectively. Assuming that the relaxation rates for the methyl probes in *A* and *B* are identical (and the same for *C* and *D*), Eq. [S13], that now includes relaxation, simplifies to

$$\frac{dM_Z^{A+B}}{dt} = -k_1 \frac{[A]+[B]}{2} M_Z^{A+B} + k_{-1} M_Z^{C+D} - \frac{M_Z^{A+B}}{T_1^{A,B}}$$
$$\frac{dM_Z^{C+D}}{dt} = k_1 \frac{[A]+[B]}{2} M_Z^{A+B} - k_{-1} M_Z^{C+D} - \frac{M_Z^{C+D}}{T_1^{C,D}} \quad [S14]$$

which is analogous to the rate equations for the simple exchange $G \underset{k_E}{\overset{k_G}{\rightleftarrows}} E$ where $k_G = k_1 \frac{[A]+[B]}{2}$ and $k_E = k_{-1}$. Note that $[A]=[B]$ since the sample was purified as double stranded DNA, *CD*.

Analysis of the 12-mer$_{Dam}$ melting experiment

We start, as above, by considering the binding reaction $A + B \underset{k_{-1}}{\overset{k_1}{\rightleftarrows}} CD$ and we define the total concentration of single DNA strands in the sample (that includes both single- and double-stranded DNA), C_{SS}, as C_{SS}=2[*CD*]+[*A*]+[*B*]. Therefore, the fractions of individual DNA strands localized to single- and double-stranded molecules are given by

$$f_{SS} = \frac{[A]+[B]}{C_{SS}}, f_{DS} = \frac{2[CD]}{C_{SS}}. \quad [S15]$$

In the melting experiments considered here where we begin with double stranded DNA (*CD*) it follows that [*A*]=[*B*]. The association constant, $K_A = \frac{k_1}{k_{-1}}$ can be written as

$$K_A = \frac{[CD]}{[A][B]} = \frac{2 f_{DS}}{C_{SS}(1-f_{DS})^2} \quad [S16]$$

and at the melting temperature, T_M, f_{DS} = 0.5 so that $K_A = \frac{4}{C_{SS}}$. Solving for f_{DS} in Eq. [S16] gives

$$f_{DS} = \frac{C_{SS}K_A + 1 - \sqrt{2C_{SS}K_A + 1}}{C_{SS}K_A}, K_A = e^{-(\Delta H - T\Delta S)/(RT)}. \quad [S17]$$

The temperature melts of Figure 3B are fit to Eq. [S17] to extract ΔH, ΔS from which T_M is readily calculated as

$$T_M = \frac{\Delta H}{\Delta S - R \ln \frac{4}{C_{SS}}}. \qquad [S18]$$

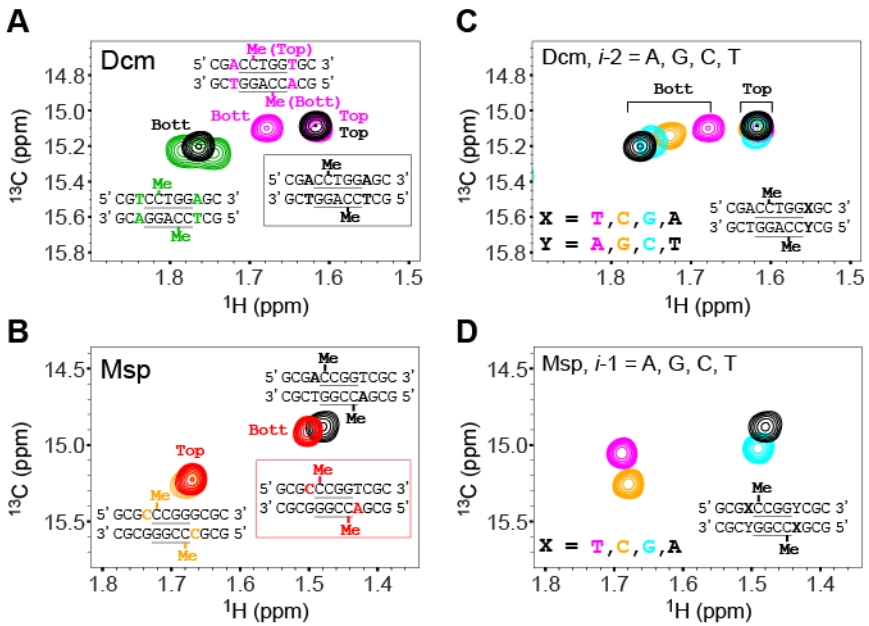

Fig. S1. Assignment of methylated oligonucleotides. (A) The Dcm MTase generates 5mC labels at C nucleobases in the top and bottom strands, 5'-CCTGG-3' and 3'-GGACC-5', respectively. In order to obtain chemical shift assignments for methyl groups in 601 DNA we have prepared a small oligonucleotide with a very similar sequence as the 'parent' 601 DNA molecule (boxed sequence, highlighted with black methyls and corresponding peaks in black; note that the *i*-2 positions are either A or T depending on the strand), along with a pair of 'symmetric' sequences in which the *i*-2 positions are either both A (pink; top and bottom strands) or both T (green). A comparison of black, pink, and green peaks provides the assignment of top and bottom methyl groups in the sequence of interest, as indicated. Pairs of peaks are observed for each of the 'symmetric' sequences, resulting from either T or A at the *i*+1 position. (B) The Msp MTase, like Dcm, produces a pair of labels, leading to the spectrum in red (boxed sequence is very similar to the 'parent' 601 DNA). As the *i*-1 positions are either C (top strand) or A (bottom) we have prepared a pair of symmetric oligonucleotides where both *i*-1 positions (top and bottom strands) are either C (orange) or A (black), from which the assignments of the top and bottom methyl groups in the red spectrum follows. Note that only single peaks are observed for each of the symmetric oligonucleotides as the *i*±1 and *i*±2 positions are identical for both top and bottom strands. (C) Overlay of four Dcm-methylated oligonucleotides, where the *i*-2 nucleobases (Y) are one of T, C, G, or A for the bottom strand, while the corresponding *i*+4 position on the top strand (X) is varied as indicated in the inset showing the sequence. There is no change in the position of the peak derived from the top strand as changing the base four positions distal from the methyl

group has no effect. However, when the base at the *i*-2 position is changed (bottom strand, Y), a clear ^{1}H downfield shift is observed from Y= A, G, C, to T, with the largest effect from A to T and smaller variations from A to G, and from C to T. (D) Demonstration of how the identity of the nucleobase at the *i*-1 position affects the chemical shifts of 5mC, showing significant downfield chemical shift changes upon substituting pyrimidines for purines at position *i*-1.

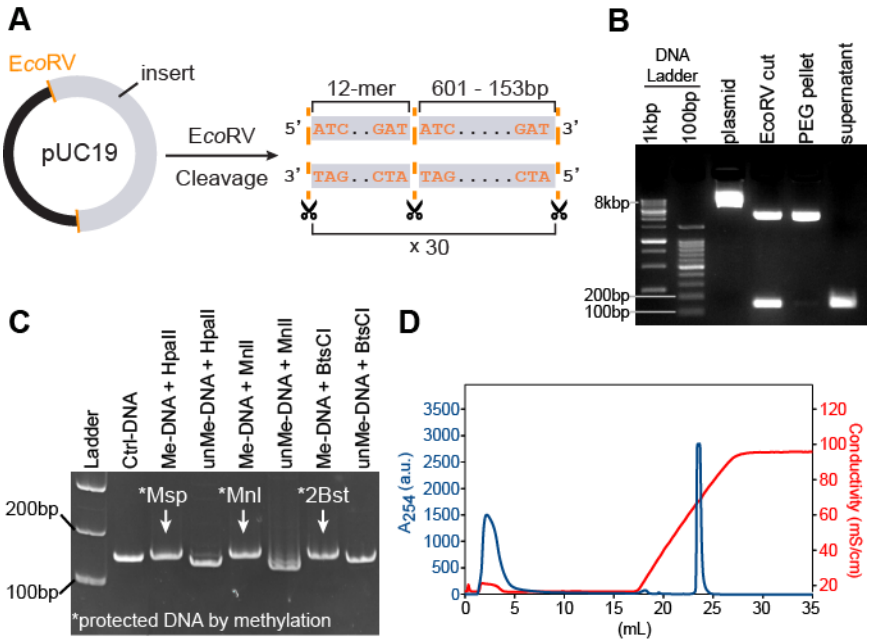

Fig. S2. 601 DNA expression and purification. (A) Schematic of the high-copy number plasmid DNA used for the expression of the 601 fragment of interest. Approximately 30 copies of the 601 sequence are inserted into a pUC19 vector, each separated by 12-bp DNA linkers (12-mer$_{Dam}$). The linker and 601 DNA segments are 'liberated' from the backbone by digestion with the EcoRV restriction endonuclease, generating separate copies of 601-DNA and of linker-DNA. For simplicity only two of the multiple EcoRV sites (orange) are shown in the plasmid. (B) DNA fractions from different purification stages resolved using 2% agarose gel electrophoresis in 1x Tris-acetate-EDTA buffer. Lanes to the right of the 'DNA Ladders' show: (column i) plasmid DNA purified using QIAGEN Giga prep columns (see above), (column ii) plasmid DNA digested with EcoRV enzyme, separating the plasmid backbone (upper band) from 601 DNA (lower band; 12-mer$_{Dam}$ is too small to be detected on this gel), (column iii) backbone pellet from PEG precipitation, and (column iv) supernatant from PEG precipitation containing 601 DNA.

(C) Digestion assays confirming that DNA methylation reactions have progressed to completion. All DNA samples have been methyl-labeled at the five sites indicated in Figure 4B. The Ctrl-DNA lane contains intact 601 DNA that has not been exposed to restriction enzymes (REs). The final 6 lanes are divided into pairs of methylated (Me-DNA) and unmethylated (unMe-DNA) 601 DNA to which have been added the corresponding REs that cleave the unMe-DNA. REs HpaII, MnlI, and BtsCI recognize the same sites as the MTases Msp, Mnl, and Bst, respectively. When the DNA is methylated, it is protected from digestion by the RE and the 601 DNA remains intact. Only the largest of the two fragments that are produced by the addition of a RE to unMe-DNA can be visualized on the gel, as the remaining fragment is too small. 7% native PAGE was run at room temperature, for 1 hr at 200 V. (D) Representative ion exchange (Mono Q column) chromatogram of methylated 601 DNA. Residuals from the methylation reaction, e.g. enzymes, are eluted first due to their low affinity for the strong anion-exchange resin. 601 DNA elution, performed using a linear gradient of NaCl up to 1M, starts at a conductivity of ~65 mS/cm, corresponding to ~0.7 M NaCl in the buffer.

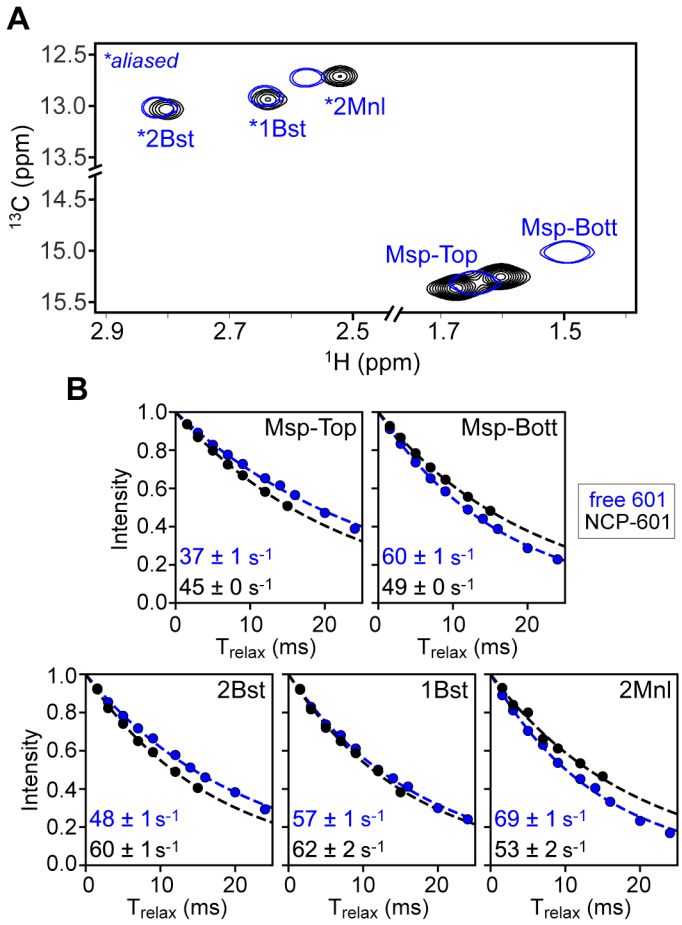

Fig. S3. Comparison of methyl spectra recorded on ^{2}H-601 Widom DNA (free 601) and ^{2}H- 601 Widom DNA as part of an NCP (NCP-601). (A) Superposition of ^{13}C-^{1}H HMQC spectra of free 601 (blue, two contours) and NCP-601 (black, multiple contours), methylated simultaneously by 1Bst, 2Bst, 2Mnl, and Msp. The assignments for free 601 are indicated in blue, and were obtained from spectra of singly and doubly (1Bst and 2Bst) methylated oligonucleotides (See Fig. 4B in main text). Assignments of NCP-601 were transferred from the free 601 spectrum. Methyl correlations derived from 6mA have been aliased; these appear at approximately 33 ppm (see Fig. 4B). (B) Methyl ^{1}H R_2 relaxation rates in free 601 and NCP-601. The decay of the slowly relaxing component of ^{1}H transverse magnetization was measured at 45°C and 800 MHz. Single exponential fits (dashed lines) of data from the five methyl groups in free (blue) and NCP-bound (black) 601 DNA samples were used to extract R_2 rates (bottom left corner).

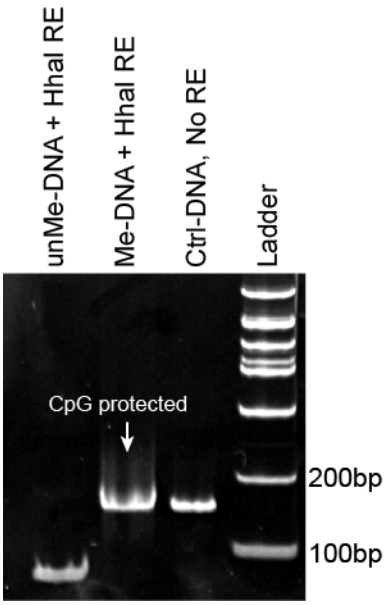

Fig. S4. Verification of CpG-methylation of 601 DNA via RE digestion. CpG-methylated and unmethylated DNAs were treated with the HhaI RE which recognizes the 5'-GCGC sequence, located in the middle of 601 DNA, cutting the DNA to generate two fragments of ~76-bp. When the CG sites are methylated, the DNA is protected from cleavage at this site. DNA fragments have been resolved on a 7% acrylamide gel.

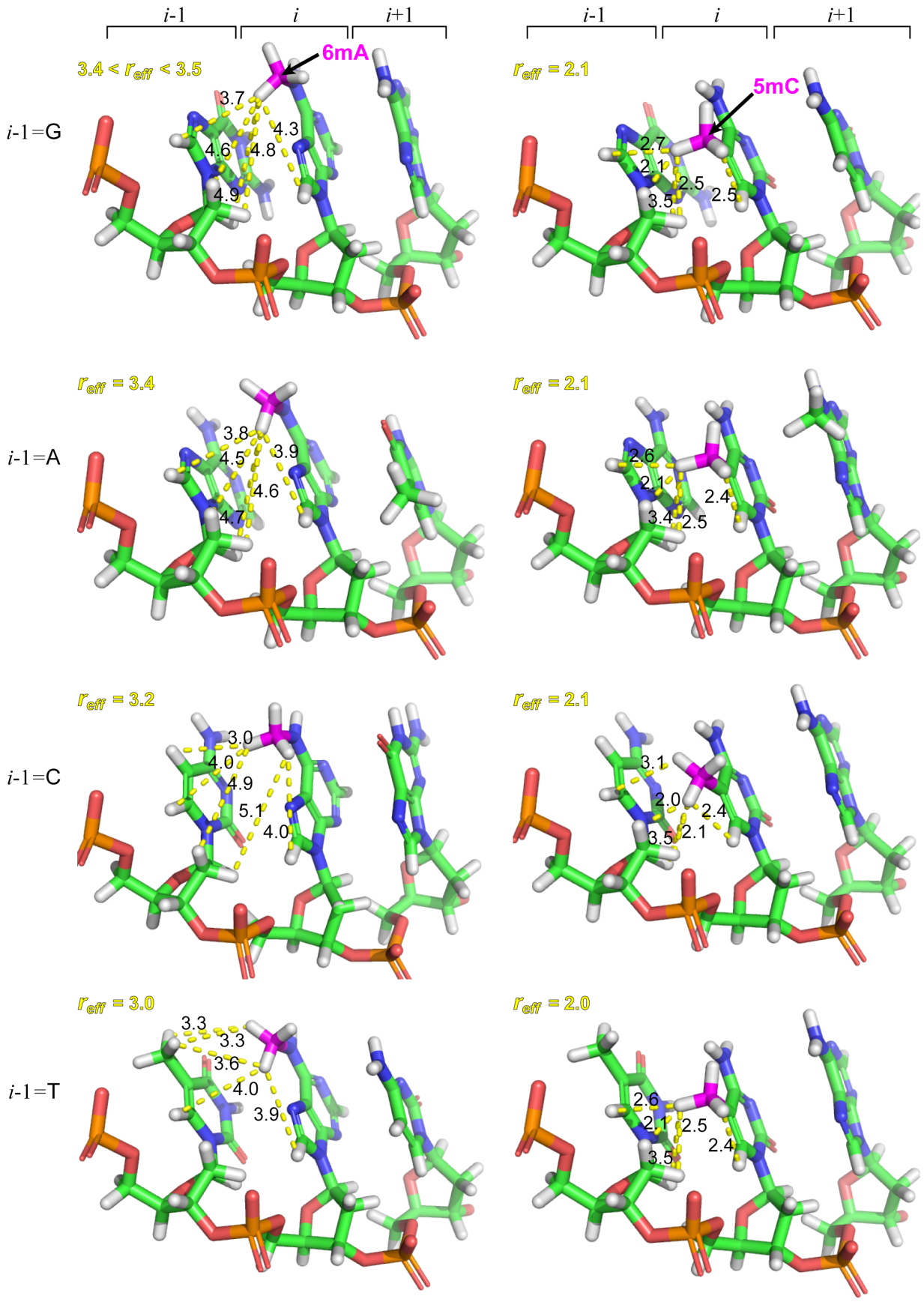
i-1
i
i+1
i-1=G
3.4 < r_eff < 3.5
6mA
3.7
4.3
4.6
4.8
4.9
r_eff = 2.1
5mC
2.7
2.1
2.5
3.5
2.5
i-1=A
r_eff = 3.4
3.8
4.5
3.9
4.6
4.7
r_eff = 2.1
2.6
2.1
2.4
3.4
2.5
i-1=C
r_eff = 3.2
3.0
4.0
4.9
5.1
4.0
r_eff = 2.1
3.1
2.0
2.4
3.5
2.1
i-1=T
r_eff = 3.0
3.3
3.3
3.6
4.0
3.9
r_eff = 2.0
2.6
2.1
2.5
2.4
3.5

Fig. S5. Segments of ideal B-form DNA structures, as in Figure 5, with methyl groups added to the N6 (6mA, left column) and C5 (5mC, right column) positions of the central A and C bases (position *i*), respectively. Yellow dashed lines connect methyl protons with the five closest neighboring protons in the structure. Each structure corresponds to a different nucleobase in the *i*-1 position, as illustrated. The slight differences in distances highlighted here and in Figure 5A are due to the fact that the orientations of the protons in the added methyl groups can be different (from the 3-fold methyl rotation). The effective distance, r_{eff}, is defined as the distance that a single proton must be placed from the 6mA or 5mC methyl group such that its contribution to relaxation is the same as that from all of the proximal non-methyl protons in the structure. It is given by $r_{eff} = \left(\frac{1}{3}\sum_{j=1=3}\sum_{q}\frac{1}{r_{j,q}^{6}}\right)^{-1/6}$, where q is a proton external to the methyl group in question and j is one of the three methyl protons. For the 6mA methyl group corresponding to *i*-1 = G there is a slight contribution from protons on the nucleobase at the *i*+1 position and the range of values listed corresponds to the deviations in r_{eff} that arise depending on whether *i*+1 is A, G, C, or T. There is no such dependence for the other methyls and hence only a single r_{eff} value is listed in these cases.

SI References

1. H. Kato, *et al.*, Architecture of the high mobility group nucleosomal protein 2-nucleosome complex as revealed by methyl-based NMR. *Proc. Natl. Acad. Sci. U. S. A.* **108**, 12283–12288 (2011).
2. J. L. Kitevski-LeBlanc, *et al.*, Investigating the dynamics of destabilized nucleosomes using methyl-TROSY NMR. *J. Am. Chem. Soc.* **140**, 4774–4777 (2018).
3. P. N. Dyer, *et al.*, Reconstitution of nucleosome core particles from recombinant histones and DNA. *Methods Enzymol.* **375**, 23–44 (2004).
4. F. Delaglio, *et al.*, NMRPipe: A multidimensional spectral processing system based on UNIX pipes. *J. Biomol. NMR* **6**, 277–293 (1995).
5. W. H. Press, S. A. Teukolsky, W. T. Vetterling, B. P. Flannery, *Numerical Recipes in C. The Art of Scientific Computing*, 2nd Ed. (Cambridge University Press, 1988).
6. V. Tugarinov, L. E. Kay, Relaxation rates of degenerate ^{1}H transitions in methyl groups of proteins as reporters of side-chain dynamics. *J. Am. Chem. Soc.* **128**, 7299–7308 (2006).
7. G. Bouvignies, L. E. Kay, A 2D ^{13}C-CEST experiment for studying slowly exchanging protein systems using methyl probes: an application to protein folding. *J. Biomol. NMR* **53**, 303–310 (2012).
8. M. Ottiger, A. Bax, How tetrahedral are methyl groups in proteins? A liquid crystal NMR study. *J. Am. Chem. Soc.* **121**, 4690–4695 (1999).
9. H. Sun, L. E. Kay, V. Tugarinov, An optimized relaxation-based coherence transfer NMR experiment for the measurement of side-chain order in methyl-protonated, highly deuterated proteins. *J. Phys. Chem. B* **115**, 14878–14884 (2011).
10. V. Tugarinov, R. Sprangers, L. E. Kay, Probing side-chain dynamics in the proteasome by relaxation violated coherence transfer NMR spectroscopy. *J. Am. Chem. Soc.* **129**, 1743–

1750 (2007).

11. N. A. Farrow, O. Zhang, J. D. Forman-Kay, L. E. Kay, A heteronuclear correlation experiment for simultaneous determination of ^{15}N longitudinal decay and chemical exchange rates of systems in slow equilibrium. *J. Biomol. NMR* **4**, 727–734 (1994).

12. J. D. Engel, P. H. von Hippel, Effects of methylation on the stability of nucleic acid conformations: studies at the monomer level. *Biochemistry* **13**, 4143–4158 (1974).

13. D. Vasudevan, E. Y. D. Chua, C. A. Davey, Crystal structures of nucleosome core particles containing the "601" strong positioning sequence. *J. Mol. Biol.* **403**, 1–10 (2010).

14. S. Bilokapic, M. Strauss, M. Halic, Histone octamer rearranges to adapt to DNA unwrapping. *Nat. Struct. Mol. Biol.* **25**, 101–108 (2018).

15. N. Tjandra, A. Bax, S. E. Feller, R. W. Pastor, Rotational diffusion anisotropy of human ubiquitin from ^{15}N NMR relaxation. *J. Am. Chem. Soc.* **117**, 12562–12566 (1995).

16. A. Sekhar, A. D. Bain, J. A. O. Rumfeldt, E. M. Meiering, L. E. Kay, Evolution of magnetization due to asymmetric dimerization: theoretical considerations and application to aberrant oligomers formed by apoSOD1(2SH). *Phys. Chem. Chem. Phys.* **18**, 5720–5728 (2016).